Charge transport in a Hubbard-Holstein junction: Preliminary results from a DFT approach

Eric Ceccarelli

LUNDS UNIVERSITET

Supervisor: Claudio Verdozzi
Co-supervisor: Emil Viñas Boström

Thesis submitted for the degree of bachelor (15 hp)

Department of Physics
Division of Mathematical Physics

June 8, 2019

Acknowledgments

First of all I would like to thank my supervisor Claudio Verdozzi for giving me a great topic. I also thank him for always being available and not taking a day off from guiding me through this project.

I would also like to thank my co-supervisor Emil Viñas Boström who was of great help when crosschecking my results and helping me improve and fix my code. I am also very grateful for the patience and perseverance of both when interpreting and checking the results which I presented, and I would like to thank Megha Gopalakrishna for a useful discussion about computational time dynamics.

Lastly I would like to thank my family and girlfriend for moral support during the most stressful weeks.

Abstract

Many-body systems are extremely complicated to describe due to mutual interactions between the constituent particles. This is for example the case of systems with electron-electron (e-e) and electron-phonon (e-ph) interactions.

Here, we consider e-e and e-ph interactions within the Hubbard-Holstein model, a very popular template to describe electron-phonon systems. Specifically, we perform an explorative investigation of the nonequilibrium (transport) properties of a Hubbard-Holstein single impurity coupled to two finite but large noninteracting 1D chains.

Such situation is addressed using Density Functional Theory (DFT), where the one-particle density of a many-body interacting system is determined in terms of a non interacting many-particle image system.

In more detail, we calculate the electronic density by solving the so-called Kohn-Sham equations, while the central ingredient of the DFT approach, the exchange-correlation potential, is obtained from a reference system using an adiabatic and local density approximation. At the same time, the phonon displacement is evaluated within the Ehrenfest approximation. This two-component (electron+phonon) Kohn-Sham system is time evolved via numerical methods.

The conduction properties of the junction are studied as a function of electron-electron and electron-phonon interactions, and of the applied bias. It is found that interactions strongly affect the conductance, mostly in the transient regime, but have relatively small influence on the steady state current.

Finally, the current calculated using DFT is also compared to a treatment based on the Ehrenfest approximation. It is found that the latter is a good approximation to the DFT result for large frequencies but not for smaller ones.

Contents

List of abbreviations

DFT- Density Functional Theory
TDDFT - Time Dependent Density Functional Theory
HH - Hubbard-Holstein
xc/XC - Exchange-Correlation
HF - Hartree-Fock
KS - Kohn-Sham
LDA - Local Density approximation
ALDA - Adiabatic Local Density Approximation

1 Introduction and Background

Quantum mechanics is vital for a microscopic description of matter, in particular for solid state physics. Many of the properties in materials are caused by quantum mechanical effects and, to accurately predict them, all the interactions in the system need to be accounted for. The problem of such an approach stands in the massive number of particles. All bodies interact with each other, rendering an exact simulation of the system extremely challenging due to the exponential growth of the Hilbert space with the number of particles. The problem simplifies substantially if the particles are treated as non interacting. However neglecting the interacting nature of the particles would lead to poor results for systems with strong interactions. To mitigate such errors, the interactions can be introduced via an effective potential in the single body problem, which is often done by introducing Density Functional Theory(DFT) [1].

The evaluation of the many body problem using the many body wavefunction can efficiently be avoided adopting DFT that, instead, considers a secondary system of non interacting particles with the same density as the interacting one. [2] The particle interactions in the secondary system is accounted for by effective potentials. This method is explained in more detail in section (2).

The time-dependent generalization of DFT, which is called Time Dependent Density Functional Theory (TDDFT), is used to describe the time evolution of systems out of equilibrium and uses the same ideas and principles as in static DFT [3]. Both DFT and TDDFT have been originally introduced to deal with realistic materials. However, they also found application in lattice models [4, 5, 6, 7], an important example of which is the repulsive Hubbard model.

The Hubbard model describes a system of interacting particles in a lattice and is used, among other things, to determine the conducting properties of systems. To also introduce electron-phonons interactions in a Hubbard lattice, the model is often extended to what is referred to as the Hubbard-Holstein model.

In general, electron-phonon interactions are particularly relevant at high temperatures and therefore have a major impact on the conductance of macroscopic samples, and understanding the role of electron-phonon interactions is of main importance in the study of high temperature superconductors [8, 9]. Another field interested in electron-phonon interactions is the semiconductor industry due to the strong effect the electron phonon interaction have on the charge mobility of a system [10].

The Hubbard-Holstein (HH) model can also be used to describe the transport in a nanoscale junction affected by electron-electron and electron-phonon interactions. Our HH system, made of a single impurity site with Hubbard-Holstein interactions coupled to two finite but large noninteracting 1D chains, is explained in more detail in section (1.3).

Using TDDFT, the current over the junction can be calculated to investigate the current transient behaviour, if the system reaches a steady state and, in that case, how such steady state is affected by different parameters such as electron-electron or electron-phonon interaction strength, hopping parameter or applied bias.[11]

However this thesis takes a more theoretical approach to the problem by performing simulations rather than analysing experimental results. The main goal of this work is to investigate the simultaneous effect of electron-electron and electron-phonon interactions on

the transport properties of a nanojunction. Our DFT approach is a rather novel approach to this type of situation; thus, our study is more explorative than systematic in character, and principally aimed to gain initially insight into the scope of a (TD)DFT description. As a result, the thesis focusses more on the development of new and revisitation of old parts of the theoretical/numerical toolkit necessary for a DFT description, rather that examining a wide range of physical situations/features (that are however well within reach of the approach).

1.1 Quantum transport

Quantum transport is an area of basic science and technology that concerns the conducting properties of non equilibrium nanoscale systems which cannot be described by classical physics [12]. In the classical regime, transport in a system can efficiently be described with with Ohm's law while, in the quantum regime, other properties such as the Coulomb blockade are present and therefore Ohms law is no longer valid. The Coulomb blockade, in mesoscopic and nanoscale physics, is the decrease of the current through a junction caused by an electrostatic barrier created by the electrons in the system [13].

Within limits, the basic transport properties of nanoscale devices can be similar at different sizes. For example, a quantum dot, composed of few atoms, can exhibit a behavior similar to a semiconductor device which consists of billions of atoms. However, to observe the effect of quantum transport in micrometer devices, temperature must be only a few Kelvin, whereas in atomic-scale devices this can be possible also at much higher temperatures. This is the result of the interplay of quantum transport energy scales and the systems internal energy scales, i.e. the voltage applied to the system, eV (or the temperature k_BT), and the transport scale determined by conductance quantum $G_Q = e^2/\pi\hbar^2$, where e is the electron charge and $\hbar$ is the reduced Planck constant.

Quantum transport is a non equilibrium phenomenon and has been studied using different approaches. One of such methods, of interest here, is provided by TDDFT [14]. A type of systems of great importance for quantum transport is quantum dots, with great potential for new technologies [15]. The model system considered in this thesis can be seen as a minimal description of a quantum dot, with electron-phonon interactions, in a transport setup.

1.1.1 Landauer formula

To investigate the quantum transport properties of nanoscale devices the Landauer formula [16] is often used. In this way, the expression for the conductance is

$$\sigma = \frac{e^2}{\pi\hbar} T \tag{1}$$

T is the transmission coefficient and $\hbar$ the reduced Planck constant. However the Landauer approach is not used in this thesis for various reasons, the main of which for us is that it would require advanced concepts such as Green's functions which are beyond the scope of this work. Furthermore, as discussed in more detail in section 3.1.1, there can be situations which require to go beyond the Landauer treatment.

We illustrate this point with a brief discussion adapted from Ref. [13]. For a junction made of a single impurity level with electron-electron interactions, and connected to two

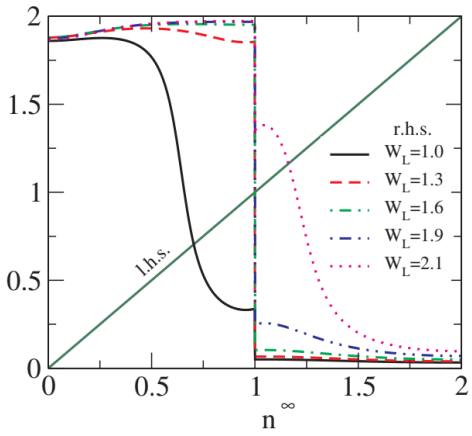

Figure 1: *Plot from Ref. [13] showing the graphical solution to the self consistent condition in equation 2 for different value of the bias* W_L.

semi-infinite leads, the steady state density at the junction must fulfill the self consistent condition

$$n^{\infty} = \sum_{\alpha=L,R} \int_{-\infty}^{\epsilon_F + W_\alpha} \frac{d\omega}{2\pi} \Gamma(\omega - W_\alpha) |G(\omega)|^2. \tag{2}$$

Here $G(\omega)$ is the retarded Green's function and $\Gamma(\omega)$ is the width function [13], but a knowledge of these concepts is not necessary.

In a (TD)DFT treatment, the Green's function in the integrand depends on the KS potential v_{KS}. The latter in turn depends on the impurity density (hence the need for self-consistency, since one is solving a highly non linear equation for the density). Since the KS potential is discontinuous at density $n = 1$, the self consistent condition does not have solutions for some values of the bias.

This concept is more easily grasped by solving this equation graphically as discussed in Ref. [13]. In figure 1, taken from Ref. [13], we see that for some values of the bias the solution to the self consistent equation 2 falls in the interval of discontinuity, i.e. we have in fact *no* solution. In the time domain, this corresponds to steady oscillations in the current and the density in the long time limit, as it can be observed in the results of the paper Ref. [13] . Thus, a time-dependent approach can be preferable in certain situations, because more general. However, the present discussion indirectly also shows that a proper use of the Landauer formula would require generalizations and tools beyond the level of this work, and this motivates the choice of the approach used here.

1.2 Density functional theory

DFT is a computational quantum mechanical method developed in the 60' by Hohenberg, Kohn and Sham. [1, 2] The key idea of DFT is to treat a many body interacting system as a non interacting one using the electron density as the main variable. The applications of this theory range from atoms, solids and molecules to nuclei and quantum fluids. This

approach is an efficient and in principle exact way to study properties of many body systems. In practice however, some approximations need to be adopted.

With DFT a many body interacting system can be treated as a non interacting system by introducing potentials that account for the interactions between particles. The expression for such potentials is derived from functionals of the density. Using this method the computational effort needed to solve the many body problem is greatly reduced. The main challenge with DFT is the calculation of these potentials since they are extremely complex and only known approximately. More specifically, the so called exchange correlation (XC) potential is the most troublesome term and is itself topic of current research.

Within DFT the many body system is mapped onto single particle problems called Kohn-Sham (KS) equations. The KS equations can be derived by considering the system as non interacting, meaning that the many body wavefunction can simply be calculated as a Slater determinant of the different single particle wavefunctions. The KS Hamiltonian is composed of two main terms, one accounting for the kinetic energy and a second one which incorporates the interactions between particles called Kohn-Sham potential. The KS potential can itself be decomposed into parts, one of which is the previously introduced exchange-correlation potential. This term accounts for the challenging interactions between particles and is therefore the most complex one. The second term, called Hartree-Fock potential, is derived using the so called Hartree-Fock approximation (see section 1.2.1). Besides the XC and the HF parts, a third contribution to the KS potential simply accounts for any external field applied to the system. In short,

$$v_{KS} = v_{Hartree} + v_{xc} + v_{ext} \tag{3}$$

The KS equations will then have the following form

$$(\hat{T} + v_{KS}[n]\hat{n})\,|\psi_i\rangle = \epsilon_i\,|\psi_i\rangle \tag{4}$$

Where $|\psi_i\rangle$ is the single particle wavefunction, T is the kinetic energy term, v_{KS} is the KS potential and ϵ_i is the energy of the particle. The density of the system at site r is calculated as

$$n(r) = \sum_i |\psi_i(r)|^2 \tag{5}$$

Ulterior approximations are adopted to simplify the density dependence of the KS potential. If to be treated exactly, the KS potential would depend on the density throughout the system but, to simplify the calculations, we approximate it to solely be dependent on the density of a single site. This approximation is called the Local Density Approximation (LDA). [2]

1.2.1 Hartree-Fock approximation

The Hartree-Fock (HF) approximation states that due to the antisymmetric nature of the fermionic wavefunctions the many-body wavefunction can be calculated as a single Slater determinant of all the spin orbitals in the system. This method accounts for the interactions between electrons in a system at the mean field level, with both direct and exchange contributions. The interaction arising from the Hartree-Fock approximation between electrons in a purely electronic Hubbard system can be thought as if the electrons with spin up are

affected by a field created by the electron with spin down. For this system the HF potential is determined by

$$v_{HF} = \sum_i U \frac{n_i}{2}, \tag{6}$$

where U is the interaction strength between electrons.

An important feature of the Hartree-Fock approximation is that the solution must be obtained self-consistently in the density.

1.2.2 Exchange correlation potential

An exchange-correlation potential for the purely electronic system can be derived by considering the Hamiltonian of a single Hubbard impurity in contact with a heat bath at inverse temperature β and chemical potential μ, [17]

$$\hat{H}_{Imp} = v\hat{n} + U\hat{n}_\uparrow \hat{n}_\downarrow \tag{7}$$

Here v is the on-site potential and U is the electron-electron interaction strength. We then create a simplified version of the Hamiltonian in which the particles are non interacting,

$$\hat{H}_s = v_s \hat{n} \tag{8}$$

To understand these two Hamiltonians, we can note that the possible configurations of the electron on the impurity are $|0\rangle, |\uparrow\rangle, |\downarrow\rangle, |\uparrow\downarrow\rangle$. In each of these cases the energy using H_{Imp} would correspondingly be $0, v, v$ and $2v + U$. Using the second simplified Hamiltonian (H_s) they would be $0, v_s, v_s$ and $2v_s$ since the particles are assumed to be not interacting.

The expectation value of the density of the system is calculated using the grand canonical partition function Z

$$\begin{aligned} Z &= \sum_i \langle\psi_i| e^{\beta(\hat{H}_{Imp} - \mu\hat{n})} |\psi_i\rangle = Tr\left[e^{\beta(\hat{H}_{Imp} - \mu\hat{n})}\right] \\ n &= \frac{Tr\left[e^{\beta(\hat{H}_{Imp} - \mu\hat{n})}\hat{n}\right]}{Z} = -\frac{1}{\beta}\left(\frac{\partial Z}{\partial \mu}\right)/Z = -\frac{1}{\beta}\frac{\partial}{\partial \mu}\ln Z \end{aligned} \tag{9}$$

Here it is useful to introduce a potential $v' = v - \mu$ since equation 9 only depends on this term ($n = n(v')$). This expression can then be inverted to find v' as a function of the density,

$$v'(\delta n) = -U - \frac{1}{\beta}\ln\left(\frac{\delta n + \sqrt{\delta n^2 + e^{-\beta U}(1 - \delta n^2)}}{1 - \delta n}\right) \tag{10}$$

where $\delta n = n - 1$ is introduced for simplicity. It is now useful to define a function $f(\delta n)$ which is

$$f(\delta n) = \frac{U}{2} + \frac{1}{\beta} ln\left(\frac{\delta n + \sqrt{\delta n^2 + e^{-\beta U}(1 - \delta n^2)}}{1 + \delta n}\right) \tag{11}$$

An important observation is that this function is odd, meaning that $f(-\delta n) = -f(\delta n)$. Finally we solve $v_{HXC} = v_s' - v'$ to find the expression for the Hartree exchange-correlation potential

$$v_{HXC} = \frac{U}{2} + f(\delta n) \tag{12}$$

Since the function $f(\delta n)$ is odd the expression for the potential v_{HXC} is

$$\begin{aligned} v_{HXC}(\delta n > 0) &= U + \frac{1}{\beta} \ln \left(\frac{\delta n + \sqrt{\delta n^2 + e^{-\beta U}(1 - \delta n^2)}}{1 + \delta n} \right) \\ v_{HXC}(\delta n < 0) &= -\frac{1}{\beta} \ln \left(\frac{\delta n + \sqrt{\delta n^2 + e^{-\beta U}(1 - \delta n^2)}}{1 + \delta n} \right) \end{aligned} \tag{13}$$

The second equation is evaluated at $\delta n > 0$, since this is numerically easier. This means that the exchange correlation potential is discontinuous at $n = 1$ and that when the density is exactly one, the potential is $U/2$ for all temperatures. The results obtained here for the purely electronic case will be an essential ingredient for the treatment where phonons are also included.

1.2.3 Time Dependent Density Functional Theory

The time-dependent generalization of DFT is the Time Dependent Density Functional Theory (TDDFT) [3]. TDDFT uses the same principle as regular DFT with the exception that the Kohn-Sham equations are now time dependent.

$$(\hat{T} + v_{KS}[n](t)\hat{n}) \, |\psi_i(t)\rangle = i \frac{\partial}{\partial t} \, |\psi_i(t)\rangle \tag{14}$$

The time dependence of the KS potential causes ulterior complications in the calculations. Since the terms composing the KS potential are dependent on the density at all times $t' < t$, the system will have an intrinsic time and memory dependence. This causes the system to be dependent not purely on the density at a certain time but on all previous points in time. Since this effect, called a memory effect, would render the system extremely more complicated an ulterior approximation called Adiabatic Local Density Approximation (ALDA) is used. With ALDA the systems properties depend entirely on the density at a specific point in time.

1.3 Hubbard-Holstein model

The naturally occurring configurations of physical systems tend to have the lowest possible energy. The same principle holds for atoms in a solid where, to minimize the interatomic interactions, their arrangement follows a regular pattern. Neglecting the possibility of imperfections, such as vacancies or irregular structures, all sites in the lattice are in an equilibrium position that is determined by the interactions with the neighbouring ones. A displacement from equilibrium will cause an oscillatory motion. In quantum mechanics the periodic movement of atoms is quantized using a quasiparticle called a phonon which allows the distinction between different vibrational modes. As temperatures increases, so does the way phonons impact the system's properties, such as e.g. conductivity. This is because the movement of atoms introduces more irregularities in the solid leading to more electron scattering.

To describe a system with electron-electron and electron-phonon interaction we use the Hubbard-Holstein model. To construct such a model the purely electronic model is first introduced (Hubbard model). This model is often used to describe properties of solid structures since it portrays the behaviour of interacting particles in the lattice.

The Hamiltonian of the Hubbard model is composed by three different terms. One representing the kinetic energy of the particles, one which describes the on-site potential and one that accounts for the electron-electron interactions. Such a Hamiltonian written in second quantization formalism reads:

$$H = -t \sum_{\langle ij \rangle \sigma} a^{\dagger}_{i\sigma} a_{j\sigma} + \sum_{i} U n_{i\uparrow} n_{i\downarrow} + \sum_{i} \epsilon_i n_i \tag{15}$$

Here $a^{\dagger}_{i\sigma}$ is the creation operator which creates an electron on-site i with spin σ and $a_{i\sigma}$ is its corresponding annihilation operator; t represents the hopping amplitude, U is the electron-electron interaction strength and ϵ_i is the potential at site i and $n_{i\sigma} = a^{\dagger}_{i\sigma} a_{i\sigma}$, with $n_i = n_{i\uparrow} + n_{i\downarrow}$.

The density of the system is found by calculating the expectation value of the density operator which requires the many body wavefunction to be known. To calculate the wavefunction we generally would need to include all possible Slater determinants that can be formed from the basis states. This is however very computationally heavy. To simplify the problem DFT is introduced. Using DFT, the density found by solving the KS equations with the exact XC potential is equal to the one of the many-body problem. The KS equation for a Hubbard system is

$$\big(- t \sum_{\langle ij \rangle \sigma} a^{\dagger}_{i\sigma} a_{j\sigma} + \sum_{i\sigma} V^{KS}_{i} \hat{n}_{i\sigma} \big) \psi_i = \epsilon \psi_i, \tag{16}$$

where V^{KS} is the KS potential that is composed of the external potential term and a Hartree-XC term $V^{KS} = V^{ext} + V^{HXC}$.

To account for the phonons the Hubbard-Holstein model needs to be introduced. The HH model is similar to its purely electronic analogue but is described by a slightly more complicated Hamiltonian because of the phonon energy and interactions. In second quantization formalism the phonon energy is $\omega b^{\dagger} b$ with ω being the oscillatory frequency and $b^{\dagger}$,b the respective phonon creation and annihilation operators. In addition to the phonon energy another term, caused by the phonon-electron interactions, is present. The complete HH Hamiltonian reads:

$$\begin{aligned} H_{HH} = & \sum_{i} (\epsilon_i - \mu) \hat{n}_i + U \sum_{i} \hat{n}_{\uparrow i} \hat{n}_{\downarrow i} - t \sum_{\langle ij \rangle \sigma} a^{\dagger}_{i\sigma} a_{j\sigma} \\ & + \sqrt{2} g \sum_{i} (\hat{n}_i - 1) \hat{x}_i + \omega \sum_{i} b^{\dagger}_i b_i + \sqrt{2} \eta \sum_{i} \hat{x}_i, \end{aligned} \tag{17}$$

where μ is the electronic chemical potential, $\hat{x}_i$ is the phonon position, g is the electron-phonon coupling strength, η is the external phonon potential. The first three terms of the Hamiltonian account for the electronic part of the system. The term $\sqrt{2} g \sum_i (\hat{n}_i - 1) \hat{x}_i$ is the electron-phonon interaction term and the remaining two terms describe the phonon energy.

When introducing the phonon in the system parameters such as the hopping term (t_{ij}), the electron interaction strength (U) and the on site potential (v) take new renormalized values. These parameters are derived in the work where DFT is applied to the homogeneous Hubbard-Holstein model using the Lang Firsov transformations. However, the detailed nature of this

procedure is outside the scope of this work. [18]

$$\begin{aligned} U^{'} &= U - \frac{2g^2}{\omega} \\ t^{'}_{ij} &= t_{ij} e^{i\sqrt{2}g(\hat{p}_i - \hat{p}_j)/\omega} \\ v^{'} &= v + (g^2 + 2g\eta)/\omega \end{aligned} \tag{18}$$

Here $\hat{p}_i$ is the phonon momentum operator at site i. When the phonon coupling strength $g = 0$, the parameter $U = U^{'}$ describes the purely electronic interaction in a Hubbard model.

The phonon position must be treated quantum mechanically, within DFT. To do this it is helpful to first think of its classical analogue, the harmonic oscillator. In this case, because of the electron-phonon interaction, the equation of motion in the classical case is the shifted harmonic oscillator. When considering the quantum mechanical case the displacement of the phonon is calculated introducing DFT. Analogously to the purely electronic system the KS potential is composed of two terms; the XC term, which for the phonon is zero [18], and the Hartree term which arises from the electron density at the phonon-site. However in this thesis we will also consider a description of phonons based on the Ehrenfest approximation.This two different treatments are more carefully explained in section 3.1.2.

1.3.1 Exchange-correlation potential for a Hubbard-Holstein site

The exchange correlation potential in presence of phonons needs to be treated differently from its purely electronic counterpart. The grand canonical Hamiltonian for a single HH site reads

$$H_I = v_I \hat{n} - \mu \hat{n} + \omega b^{\dagger} b + U \hat{n}_{\uparrow} \hat{n}_{\downarrow} + \sqrt{2} g \hat{x} (\hat{n} - 1) + \sqrt{2} \mu \hat{x} \tag{19}$$

Using a similar method as for the purely electronic case, and the renormalized values for electron-electron interaction strength and potentials from equation 18, the following expression for the exchange correlation potential for a single HH impurity can be calculated. [18]

$$v_{XC}(n, x) = (1 - \delta n)\frac{U^{'}}{2} + \frac{g^2}{\omega}\delta n + \frac{1}{\beta} ln \frac{\delta n + R}{1 + \delta n}. \tag{20}$$

Here $R = \sqrt{e^{-\beta U^{'}}(1 - \delta n^2) + \delta n^2}$. When $g = 0$ we get back the expression for the purely electronic Hubbard model. The first term in the expression utilizes the renormalized interaction strength $U^{'} = U - \frac{2g^2}{\omega}$ meaning that the phonon coupling will decrease the on-site electron-electron interactions. For a positive $U^{'}$ the exchange-correlation potential will be discontinuous at $n = 1$. If $U^{'} < 0$ the discontinuity is instead at $n = 0$ and $n = 2$.

The phononic potential is derived with the same method as for the electronic one but has a simpler expression

$$\mu_{HXC} = g(n - 1) \tag{21}$$

This is just the Hartree potential arising from the electron-phonon interactions, meaning that the exchange-correlation potential for the phonon is zero [18].

In general, the exchange-correlation potential is a highly complicated object and is the main subject of many different studies, however the focus of this thesis is not on new developments concerning the XC potential, but rather on its use to investigate other properties of a HH system.

1.4 Ehrenfest Theorem

The Ehrenfest theorem relates the time derivative of the expectation value of a quantum mechanical operator with the expectation value of the commutator between the same operator and the Hamiltonian of the system.

$$\frac{\partial}{\partial t}\langle A\rangle = i\langle[H,A]\rangle + \left\langle\frac{\partial A}{\partial t}\right\rangle \tag{22}$$

This expression is extremely useful for the implementation of the phonons part in the Hubbard-Holstein system. Replacing the operator A with the momentum operator of the phonon p and considering the HH Hamiltonian in equation 22 we note that the momentum operator commutes with most terms giving the expression

$$\frac{\partial}{\partial t}\langle p\rangle = -\omega\langle x\rangle - \sqrt{2}g(\langle n\rangle - 1) \tag{23}$$

We have now found an equation of motion for the phonon, valid in DFT, without solving the KS equations for it; this equation however only holds if we deal with averages. The phonon position can then be time evolved using numerical methods such as the Verlet algorithm.

1.5 Verlet algorithm

The Verlet algorithm is often used in classical molecular dynamics to predict the motion of particles. In this thesis it is used to integrate the equation of motion for the phonon so that its position can be calculated during the time evolution.

There are several versions of the Verlet algorithm. The one considered here is obtained considering two Taylor expansions of the position $x(t)$. The first is forward in time, at $x(t+\Delta t)$, and the second backwards, at $x(t-\Delta t)$ [19].

$$\begin{aligned} x(t+\Delta t) &= x(t) + \dot{x}(t)\Delta t + \frac{1}{2}\ddot{x}(t)\Delta t^2 + \frac{1}{6}\dddot{x}(t)\Delta t^3 + O(\Delta t^4) \\ x(t-\Delta t) &= x(t) - \dot{x}(t)\Delta t + \frac{1}{2}\ddot{x}(t)\Delta t^2 - \frac{1}{6}\dddot{x}(t)\Delta t^3 + O(\Delta t^4) \end{aligned} \tag{24}$$

Summing the expressions in equation 24, and denoting the acceleration by $a(t)$, gives the final equation for the Verlet algorithm

$$x(t+\Delta t) = 2x(t) - x(t-\Delta t) + a(t)\Delta t^2 + O(\Delta t^4) \tag{25}$$

With this equation the particle motion at all times is obtained from the particle's initial position and its acceleration. The error associated with the algorithm is of the order of Δt^4.

The velocity can then be calculated from the knowledge of the trajectory

$$v(t) = \frac{r(t+\Delta t) - r(t-\Delta t)}{2\Delta t} + O(\Delta t^2) \tag{26}$$

However the error for this expression is of the order of Δt^2.

2 Method

To study the effect electron-phonon and electron-electron interactions have on the conductance of a junction, numerical simulations of a system with a single Hubbard-Holstein impurity are run for different parameters. This section presents the methodology utilised to perform simulations of the system, schematically shown in figure 2.

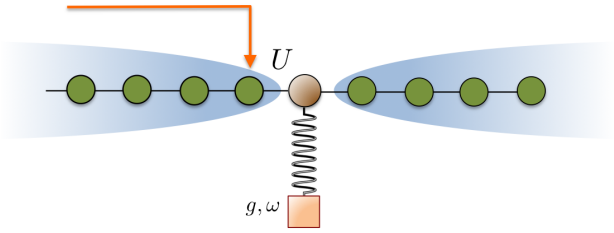

Figure 2: *A schematic rendering of the system.*

Before initiating the time evolution, one first solves self-consistently the KS equations for an initial Hubbard-Holstein Hamiltonian to find the ground state. This is always done by repeated numerical diagonalization of the KS Hamiltonian. The system is then time evolved by numerically implementing the time-dependent KS equations and the phonon dynamics. For the electrons, the dynamics was obtained in two ways: for small systems, by exact numerical diagonalization; this was done primarily for code-testing purposes. For large systems, i.e. for production runs, we used a different technique, i,e short iterated Lanczos method, which offers faster computations allowing the study of larger and more complicated systems. A description of the Lanczos method is outside the scope of this work, and can for example be found in [20]. For the phonon dynamics, in all cases the Verlet algorithm was used.

2.1 Interaction Hamiltonian

To describe the system the Holstein-Hubbard Hamiltonian is first defined. Since we assume the chemical potentials for the phonon and electrons to be zero the Hamiltonian simplifies to

$$\begin{aligned} H_{HH} =& \epsilon_i \sum_i \hat{n}_i + U \sum_i \hat{n}_{\uparrow i}\hat{n}_{\downarrow i} - t \sum_{\langle ij\rangle\sigma} a^\dagger_{i\sigma} a_{j\sigma} \\ &+\sqrt{2}g \sum_i (\hat{n}_i - 1)\hat{x}_i + \omega \sum_i b^\dagger_i b_i \end{aligned} \tag{27}$$

According to the time independent KS equations the energy states of such a Hamiltonian can be found solving the following equation

$$\hat{H}_{KS} \left|\psi_i\right\rangle = E_i \left|\psi_i\right\rangle , \tag{28}$$

where E_i is the energy corresponding to the wavefunction $|\psi_i\rangle$. The number of possible energy states will be equal to the number of sites in the system. For example a system with four sites and a single electron will have four possible configurations which are defined as $|1\rangle, |2\rangle, |3\rangle, |4\rangle$.

To find the ground state the KS Hamiltonian needs first to be set into matrix form and then diagonalized. The KS ground state is obtained by populating the N orbitals with lowest energy, where N is the number of particles. The density at site i is then calculated as

$$n_i = \sum_{k=1}^{N} \mid \psi_k(i) \mid^2 . \tag{29}$$

The ground state of the system needs to be found self consistently due to the Kohn-Sham and phononic potentials dependence on the electron density and phonon coordinate. To achieve self consistency initial values for the KS potential and the phononic displacement x are guessed. The density is then calculated by diagonalization and new values for the phonon displacement and KS potential are found. If the newly calculated displacement and density are the same as in the previous iteration to fixed accuracy criterion, self consistency is reached; otherwise new values are calculated and the procedure repeated until self consistency is obtained.

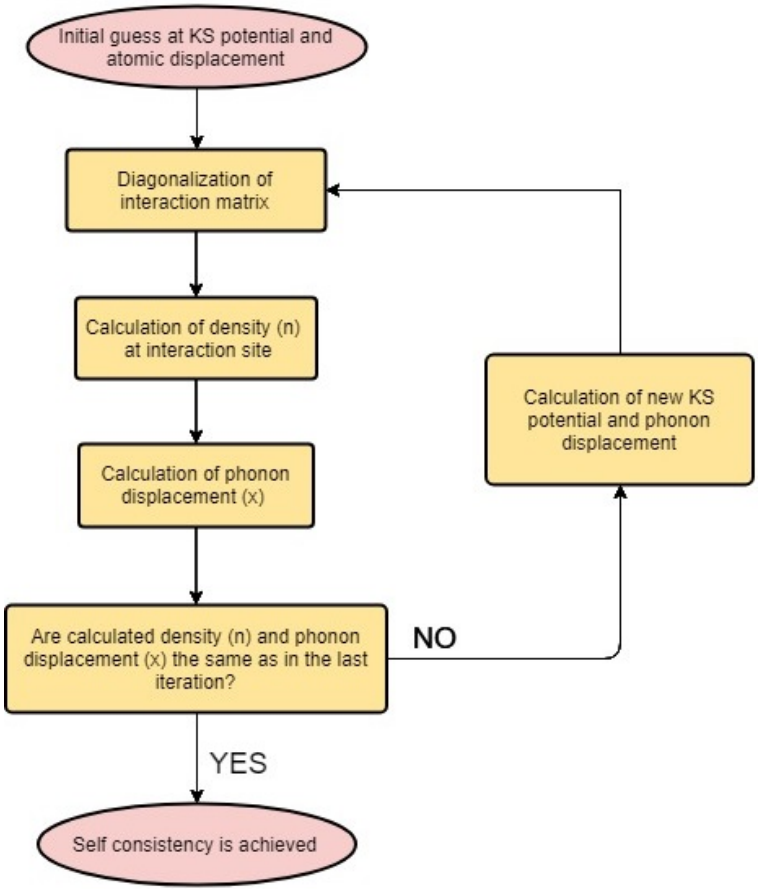

Figure 3: *Flowchart showing the iteration procedure to achieve self consistency*

2.2 Time evolution

To study the time-dependent current the system must be time evolved, which is done by solving the time-dependent Shrödinger equation

$$|\psi(t)\rangle = e^{-i\hat{H}t} |\psi_0\rangle \,, \tag{30}$$

where $|\psi_0\rangle$ is a Slater determinant of occupied KS orbitals.

Unless any bias is applied the electrons do not move from their original state meaning that the wavefunctions, and therefore the density, would not change in time. A bias is therefore applied to the system during the time evolution to create a non equilibrium system.

It is now useful to introduce a perturbed Hamiltonian $\hat{H}'$ that describes the system with the applied bias. By considering all the eigenvectors and eigenfunctions of the Hamiltonian $\hat{H}'$, and inserting the completeness relation for the perturbed Hamiltonian $\hat{H}'$, it is possible to find an expression for equation 30 without operators

$$\psi_n(t) = \sum_\lambda e^{-i\epsilon^\lambda t} \psi_n^\lambda \big(\sum_m \psi_m^\lambda \psi_m^0 \big) \tag{31}$$

Here ψ^λ satisfies $\hat{H}' \left|\psi^\lambda\right\rangle = \epsilon^\lambda \left|\psi^\lambda\right\rangle$. This equation is only valid if the perturbed Hamiltonian H' is constant in time. If instead it is time-dependent the wavefunction is evaluated after each time step.

$$\psi((n+1)\Delta) = e^{-i\hat{H}_{KS}(n\Delta + \frac{\Delta}{2})\Delta} \psi(n\Delta) \tag{32}$$

Where Δ is the time step and $n = 1, 2, 3...$ The Hamiltonian is taken at $(n\Delta + \frac{\Delta}{2})$ to have more accurate calculations according to the midpoint formula. This equation requires to create a new matrix $\hat{H}$ and to diagonalize it for each time step which leads to many calculations. To reduce the required time to run a simulation the Lanczos algorithm is used.

2.2.1 Phonon interactions

Because of the dependence of phonon displacement on the density, and of the KS potential on x, a new position x needs to be calculated after each time step. This is done using the equation of motion derived using the Ehrenfest theorem (equation 23) and the Verlet algorithm (equation 25)

$$\begin{aligned} a &= -\omega x - \sqrt{2} g(n-1) \\ x_{i+1} &= 2x_i - x_{i-1} + a\Delta t^2 \end{aligned} \tag{33}$$

To find the phonon displacement at the first time step (x_1) two initial values are needed: x_0 and x_{-1}. These values are set as the self consistent phonon displacement of the initial state. The acceleration a is simply calculated using the first equation and inserted in the Verlet algorithm for each time step.

Using this procedure the phonon displacement can be calculated in an iterative manner allowing the study of the time evolution of the system.

2.2.2 Hartree and exchange-correlation potentials

The method used for the calculation of the electron-electron interaction potentials is similar to the one used for the phonon displacement. The main difference is that these potentials are not dependent on their previous values but solely on the density at that specific time step.

The potentials are calculated using equation 20 from the density at each time step

$$v(n,x) = (1-\delta n)\frac{U^{'}}{2} + \frac{g^2}{\omega}\delta n + \frac{1}{\beta} ln \frac{\delta n + R}{1+\delta n} \tag{34}$$

The new potentials are then inserted in the Hamiltonian to continue the time evolution.

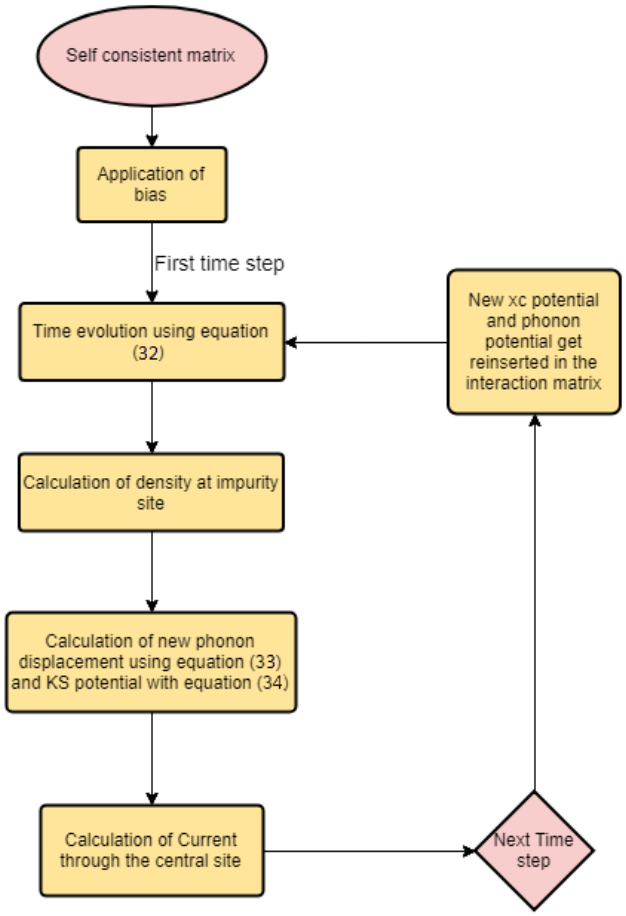

Figure 4: *Flowchart showing the time evolution procedure.*

2.3 Current

The expression for the current is derived from the continuity equation

$$\frac{d\rho}{dt} + \nabla \vec{J} = 0, \tag{35}$$

where $\vec{J}$ is the current and ρ is the electron density. By using Heisenberg equation of motion the divergence of the current is calculated to be proportional to the commutator between the density operator and the system's Hamiltonian. All of the terms in the Hamiltonian commute with the density operator except for the kinetic energy term for the electrons. The current through the central atom which is at position r is then:

$$\frac{\partial n_r}{\partial t} = i[H, n_r] = -iV((a_r^\dagger a_{r-1} - h.c.) - (a_{r+1}^\dagger a_r - h.c.)) = \hat{J}_{r+1/2} - \hat{J}_{r-1/2} \tag{36}$$

To find the value of the current the expectation value of this operator is calculated resulting in the final expression for the current,

$$J = 2V \, \mathrm{Im}\langle\psi(t)|a_{i+1}^+ a_i|\psi(t)\rangle \tag{37}$$

where $\psi(t)$ is the KS Slater determinant at time t and V is the hopping parameter. The current is evaluated on the central atom by summing up all the contributions from each occupied KS state multiplied by a factor 2 to account for spin projection.

2.4 Computer code

The computer code for this project was created from scratch in Python and at later stage a Fortran version was also produced. The latter was in part based on a pre-existing code used to study the behaviour of the current in a purely electronic non interacting system. This early Fortran version already made use of a Lanczos time propagation scheme. In both Python and Fortran codes, the electron-phonon interaction and the Verlet dynamics were introduced from scratch, while the expression for the electronic exchange correlation potential was taken from another code used in a recent DFT paper on the HH model. [18].

3 Results

In this section the results of simulations are analyzed and compared to exact results. The simulations are run to study the effect different parameters have on the steady state current through a junction. This is done by comparing the dependency the current has on the applied bias for different parameters such as electron-phonon and electron-electron interaction strengths. It is worth mentioning here that during the development of the code, the results were cross-checked with the purely electronic case as e.g. described in [11]. The code was also tested against one used in the DFT study of an HH system [18]. Additional checks were also performed to validate the implementation of the Verlet dynamics. Some of these benchmarks are reported here.

3.0.1 Verlet algorithm

To test the numerical stability and accuracy of the Verlet dynamics, the algorithm was applied to the case of a simple harmonic oscillator, and the results compared to the exact analytical solution $x(t) = A\cos(\omega t - \phi)$, where ω is the frequency, A is the amplitude and ϕ is the initial phase.

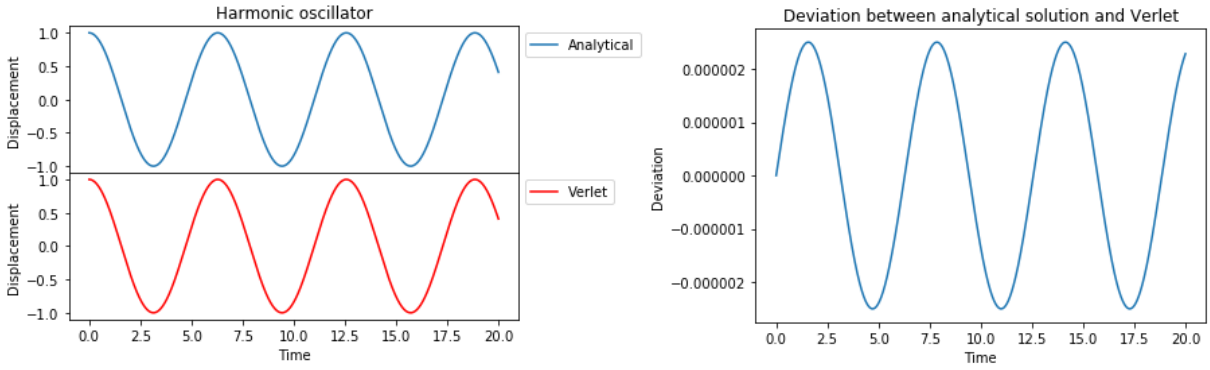

Figure 5: *The analytical solution for a simple harmonic oscillator compared to the result calculated using the Verlet algorithm. The left figure shows the displacements for the different approaches while the right figure reports the deviation between the two plots. The frequency is* $\omega = 1$

The deviation shown in figure 5 is of the order of 10^{-6} but, instead than deteriorating with time, it has an oscillatory behaviour, due to the algorithm's good numerical stability and symplectic nature [19].

3.0.2 Steady state transport

With the constructed code part of the results from the paper on steady-state transport in nanoscale conductors [11] were recreated with high accuracy. To generate the current an opposite bias was applied to each side of the junction and the current evaluated over time for different atomic chain lengths.

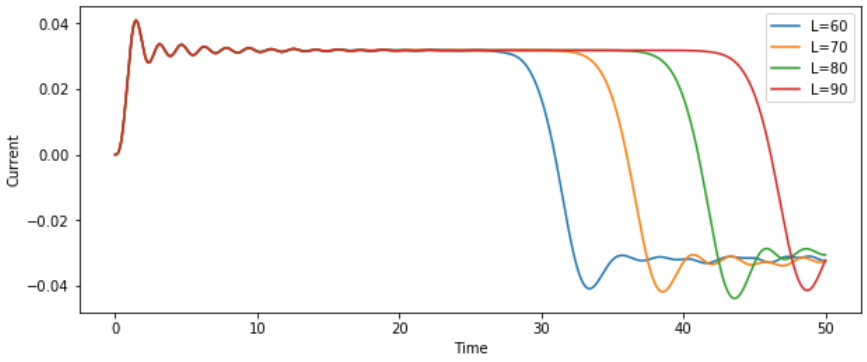

Figure 6: *The current through the junction is plotted over time for different chain lengths of L atoms. The used bias is $V = 0.1$.*

The current reaches a quasi-steady state until it drops to a negative value, as shown in figure 6. This behaviour is caused by the electrons reflecting upon the end of the chain, therefore generating a negative current. It is noted that for larger chains the quasi-steady state remains stable for longer times

3.0.3 Comparison to an existing DFT code

The developed DFT code was further cross-checked by applying it to another Hubbard-Holstein system for which DFT results were available [18]. The system considered was an eight-site chain with an HH impurity at the first site. A negative bias was applied to the impurity at time zero and then released suddenly at the first time step. The particle density at the first site was evaluated in time and the results from our code and those obtained from the other code used in [18] compared.

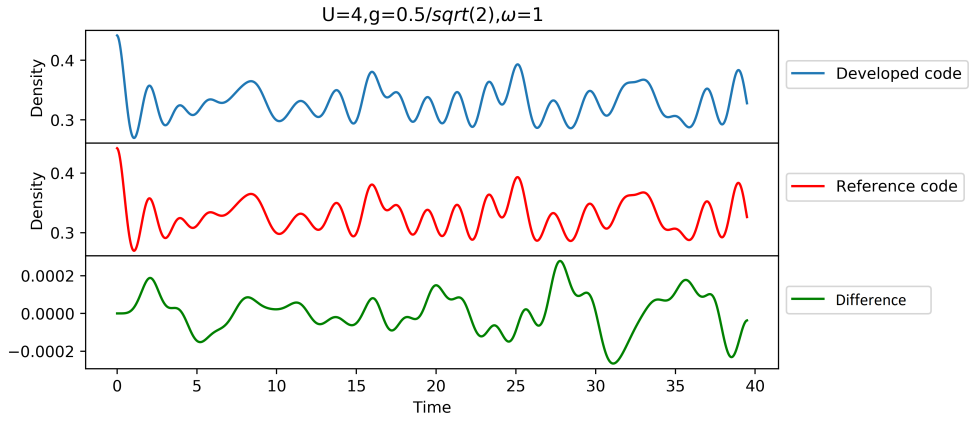

Figure 7: *Comparison between the developed code and the one used in [18] (reference code). The system is an 8 atom long chain with a Hubbard-Holstein impurity at the first site. The parameters are $U = 4, g = 0.5/\sqrt{2}$ and bias=-1. The bias is applied at time zero and released suddenly at the first time step. The image shows the density at the impurity site for the two codes and their difference.*

We note that the deviation of the results from the two codes is of the order of 10^{-4} and has an oscillatory behavior. For a purely electronic system (i.e. $g = 0$) the two codes agreed to machine accuracy, meaning that the divergence arises from the different treatment of the phonon dynamics.

3.1 Simulations

In this section the results of the quantum transport simulations are reported as well as their analysis. The simulations are for different parameters such as number of sites, number of electrons, electron-phonon coupling strength or electron-electron interaction strength.

The system is always at quarter filling meaning that the number of electrons with spin up and down is a quarter of the number of sites. The reason for the system to be considered at quarter filling is to avoid the discontinuity of the exchange correlation potential at half filling, which is known to produce artificial oscillatory behavior [13]. The main focus of the simulations is in achieving a quasi-steady state for the current and investigating the effect different parameters have on it.

The junction, which is a single HH impurity site, is placed in the middle of a 1000 atoms long chain (see figure 2). The ground state of the unperturbed systems is reached via self consistency. After that, the system is time evolved with a constant bias applied. The current is examined for different values of the bias.

In figure 8 the time-dependent current, phonon displacement and electron density at the impurity site induced by a bias $(V) = 0.5$ are presented. In all what follows, the bias is applied only to the sites left to the HH impurity (see the arrow in figure 2). Examining the current and the density, fast oscillations can be observed for short times, i.e. in the transient regime. During these oscillations, the currents overshoots above its steady state value. The oscillations, which are also present in the non interacting case, get modified by electron-electron interactions (they are greater for strong electron-electron coupling strength, e.g. for $U = 4$), but get damped relatively early in the time evolution. On the other hand, the oscillations caused by the phononic movement, get damped only at very long times.

We can observe that the main factor affecting the value of the steady state current is the electron-phonon coupling strength g. The current is smaller for greater values of g and vice versa. The reason for this strong dependence would be that the phonon displacement negatively affects the conductance of the junction and a strong electron-phonon interaction strengthen this effect. To further validate this assessment, one can look at the influence the phonon frequency has on the steady state current. We see, that decreasing the value of the frequency, the current is smaller. The combination of parameters which has the strongest effect on the current is then a strong interaction g together with a small frequency ω. In this regime the current is extremely small: In this case the relation between the displacement and frequency results in a trapping potential at the junction which hinders other charges to flow through it. To have a better understanding of these effects, in the next section we consider the estimated steady state currents for different values of the bias.

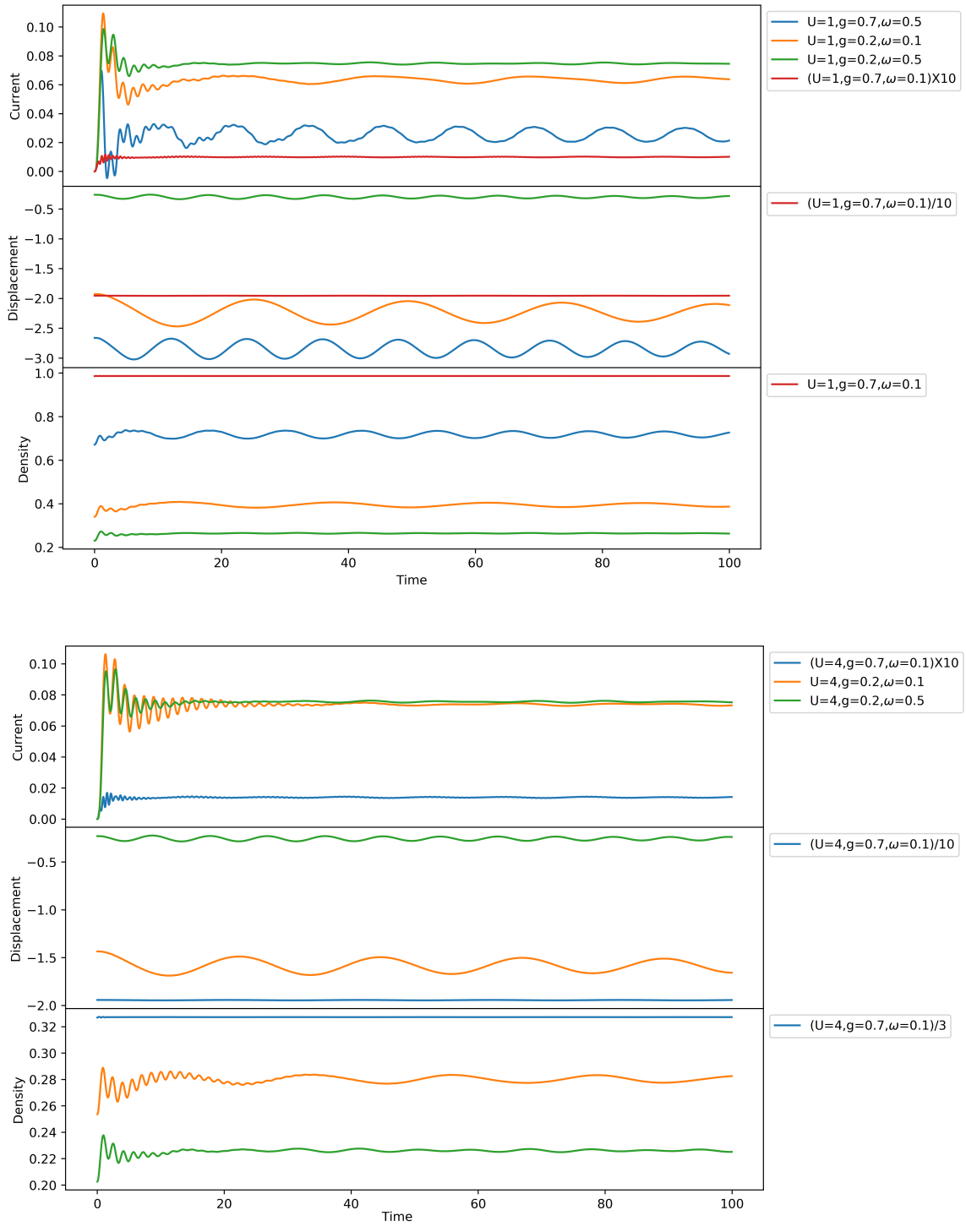

Figure 8: *Current, displacement and electron density at the impurity site as a function of time for different combinations of parameters. The curves for the parameters* $U = 4, g = 0.7, \omega = 0.1$ *are multiplied or divided by a factor of 10 to fit with the rest of the results. In all panels, the bias is* $V = 0.5$.

3.1.1 IV plots

It can be useful to start this section with few remarks on how the steady-state current is determined. The true steady state current, where the phonon oscillations have fully damped, can be obtained by i) propagating the system at very long times (much longer than those shown in the figures below) or ii) via the Landauer formula, suitably modified to account for the self-consistent phonon elongation and for the electronic correlations. For i), progressively much larger chains could be required, to avoid reflection effects, and this would become numerically prohibitive for slowly damping oscillations. Some help here would come from an adiabatic (i.e. slow) switch on of the bias. We have in fact checked that for slowly ramped bias, the oscillation are greatly reduced, while still occurring around the same average value (this shows that, at least for the cases considered, the steady state is unique, i.e. independent from the bias switch on rate.). A conceptually and practically better way would be to contact the impurity to semi-infinite leads. This can be done, see e.g. [14, 21, 13], but it requires theoretical notions beyond those developed in this thesis. Strategy ii) gives direct access to the steady state, without time evolution. However, as already discussed earlier in this thesis, in some regimes (notably for densities around half-filling) the system can have everlasting oscillations induced by a discontinuous XC potential, and these cannot be captured by the Landauer formula (so one anticipates that a self-consistent steady state solution could not occur). The investigation of this interesting aspect is left to a future study. We finally mention the forces exerted by the electronic currents on the nuclear/phonon coordinates can lead to regimes of negative friction [22], where the nuclear motion (or phonon dynamics) could stabilise in self-limiting cycles, and a steady current would not settle in. How this should be reinterpreted within a DFT description, is also left to future work. In what follows, while remaining aware of the previous considerations, we assume that a steady state exist, and the average value of the long-time limit of the oscillation gives a good estimate of it.

The steady state current is examined for different values of the applied bias using eight different combinations of parameters. The value of the current is estimated by calculating its time average at large times in the plots, as discussed before. One set of parameters ($U = 4, g = 0.7, \omega = 0.5$) is however not included in figure 9, due to some numerical instabilities which caused the current and electron density to have unreliable values.

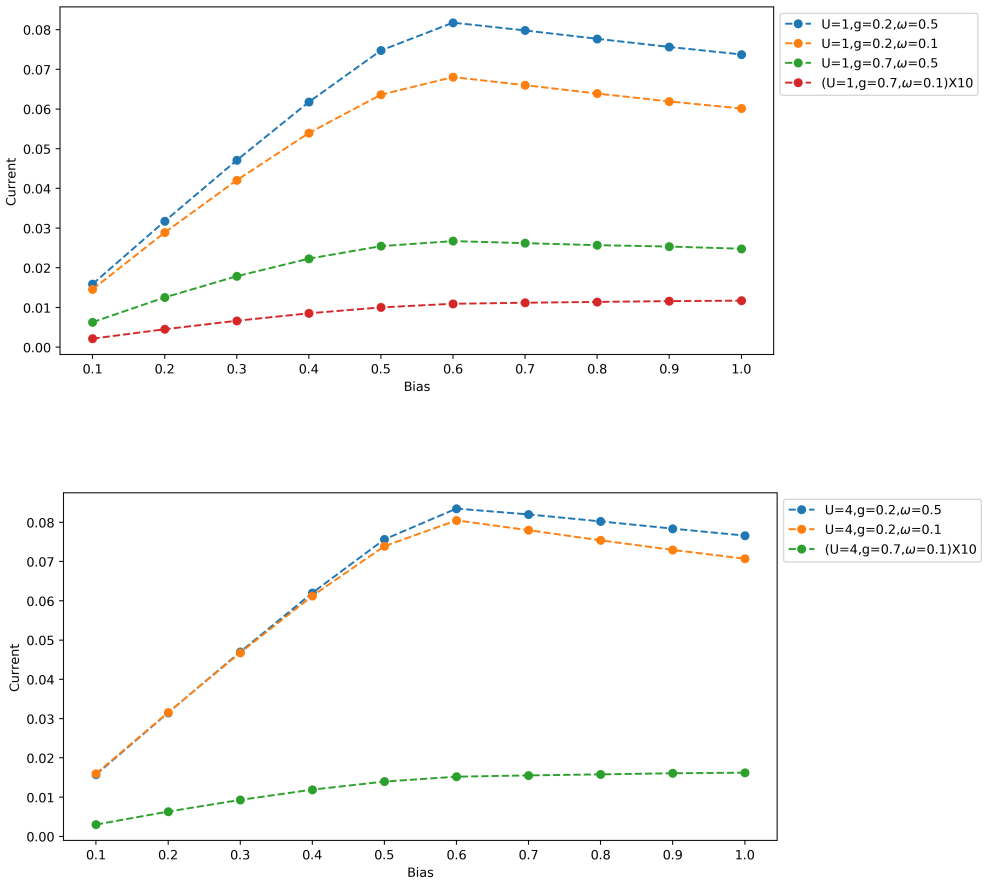

Figure 9: *Steady state current as a function of bias, for different values of* U, g *and* ω*. The current for the parameters* $U = 1$ & $4, g = 0.7, \omega = 0.1$ *is multiplied by a factor 10 to show its behaviour in the same plot as for the other parameters.*

It is found that the current follows the same trend for all parameters. It increases linearly with the bias up to $V = 0.5$ after which it starts a non-monotonic behaviour at $V = 0.6$. This effect is caused by the fact that for a large bias the available density of states in the left lead diminishes. This happens at $V = 0.6$ because for this value the bottom of the band in the left lead is above the Fermi level in the right one and therefore the overlap is lost. This can be shown by calculating the Fermi energy for the band.

$$E_F = E_0 - 2t\cos(k_F) \tag{38}$$

Here E_F is the Fermi energy, t is the hopping parameter and k_F indicates the systems filling. Since $E_0 = 0$ and at quarter filling $k_F = \frac{\pi}{4}$, the Fermi energy is $E_F = -\sqrt{2} \approx -1.4$. With no applied bias the bottom of the band is -2. When $V = 0.6$ is applied to the left lead, the bottom of the band in the left lead is now $E = -2 + 0.6 = -1.4$ which is the Fermi energy in the right lead. This has a negative effect on the conductance.

To further illustrate this behaviour we can plot the density of states for one of the systems, in figure 10 we display the density of states for a 1000 atom chain with parameters $U = 4, g =$

$0.1, \omega = 0.1$. Since the system is at quarter filling, the occupied region is the highlighted one. We can observe that the Fermi energy is -1.4 and that the bottom of the band is -2. The difference between these two values is 0.6 which is the bias at which the discontinuity happens.

The most apparent observation from figure 9 is that the current for the parameters $U = 1 \quad \& \quad 4, g = 0.7, \omega = 0.1$ is far smaller than the one for the other cases. This can be understood examining the potential, and therefore the density, at the impurity site for this set of parameters and comparing it with the one for the others cases.

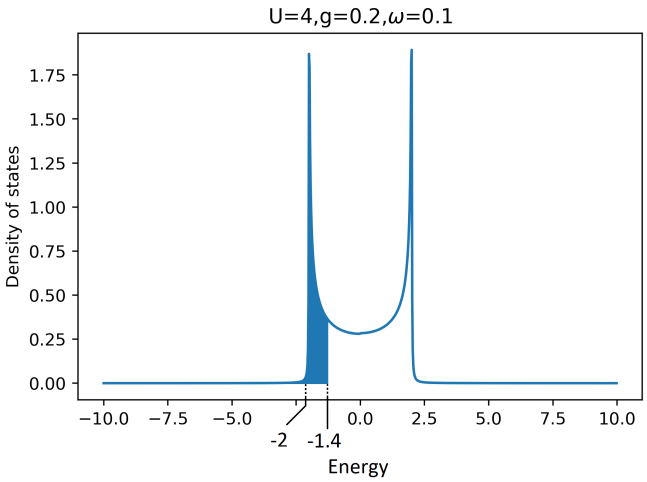

Figure 10: *Density of states for a 1000 sites system at quarter filling with parameters* $U = 4, g = 0.2, \omega = 0.1$. *The marked region represents the occupied states.*

The density for the system in its ground state is calculated from the self consistent matrix before applying the bias. The density at the impurity is proportional to the potential due to phonon and electron interactions.

For a low frequency ($\omega = 0.1$) the phonon coordinate is easily stretched and therefore it assumes a greatly negative value. This causes a strongly attractive potential at the impurity site leading to a great density especially for strong electron-phonon coupling strengths. This can be observed from the bottom panel of figure 11 where the density at the impurity site is much larger than for the other parameters.

Comparing the results shown in figure 11 to the bottom panel in figure 9 we can find some correlation. The highest current is found for the parameters which also give the smallest density at the impurity site ($U = 4, g = 0.2, \omega = 0.5$) and analogously the lowest current is found for ($U = 4, g = 0.7, \omega = 0.1$) which give the highest density.

For the parameters that give a high density at the impurity, the electrons encounter a barrier at the junction due to the strongly attractive potential. This causes the conductance of the system to drop proportionally to the effective on-site potential.

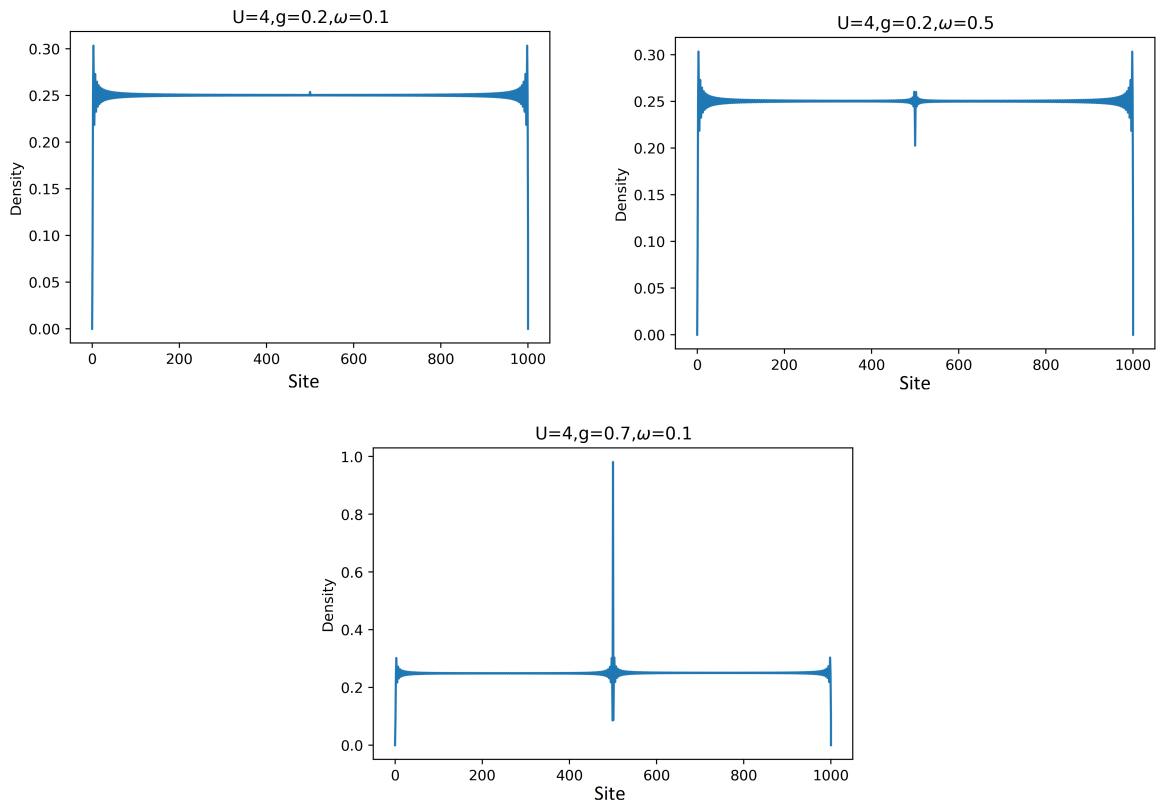

Figure 11: *Density at each site of the system after reaching self consistency, for different values of the parameters U, g and ω. The density is per channel and the system is at quarter filling.*

3.1.2 Ehrenfest approximation

In this section we briefly compare the steady state current calculated using DFT with the one using the Ehrenfest approximation for the phonons. The motivation behind this comparison is that, at present, still many calculations in transport and molecular dynamics make use of the Ehrenfest approximation, so it is quite useful how the latter performs compared to DFT, that in a way represents the next level of sophistication, while still not resorting to a full many-body treatment of the electron-phonon interaction. The system is a 400 site long chain with the HH impurity at the central site. The bias is applied adiabatically up to 0.5 on the left lead. With the Ehrenfest approximation the exchange correlation potential is calculated using the electron-phonon interaction strength $g = 0$, since this factor arises only with a full quantum mechanical treatment.

We observe that the Ehrenfest approximation is in good agreement with DFT for large phonon frequencies ω, while for small frequencies the steady state current has a much lower value than for DFT. This is caused by the fact that using DFT for small frequencies the factor $\frac{g^2}{\omega}$ has a great effect on the exchange-correlation potential v_{XC} (equation 20) via the renormalized electron-electron interaction strength $U^{'}$ (equation 18). Using the Ehrenfest

approximation, such $\frac{g^2}{\omega} = 0$, and it therefore there is no impact on the systems conductance.

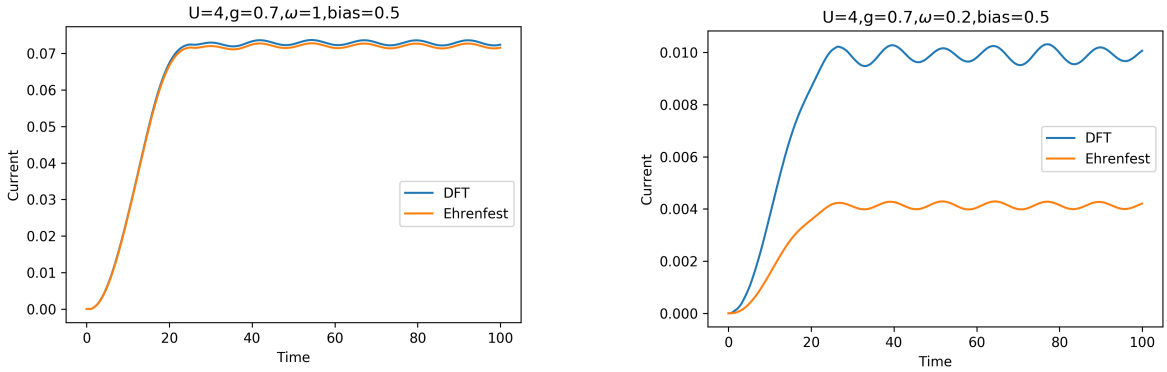

Figure 12: *Current calculated using DFT compared to the current calculated with the Ehrenfest approximation, for two different frequencies ω. The bias is 0.5 and is applied adiabatically.*

The Ehrenfest approach was compared to DFT for two other set of parameters ($U = 1, g = 0.2, \omega = 0.5$ & $U = 1, g = 0.7, \omega = 0.1$) by creating IV plots. The result is in agreement with what could already be observed in figure 12. For large frequencies the Ehrenfest approach offers a relatively accurate approximation while for small ones the difference between the two approaches is substantial.

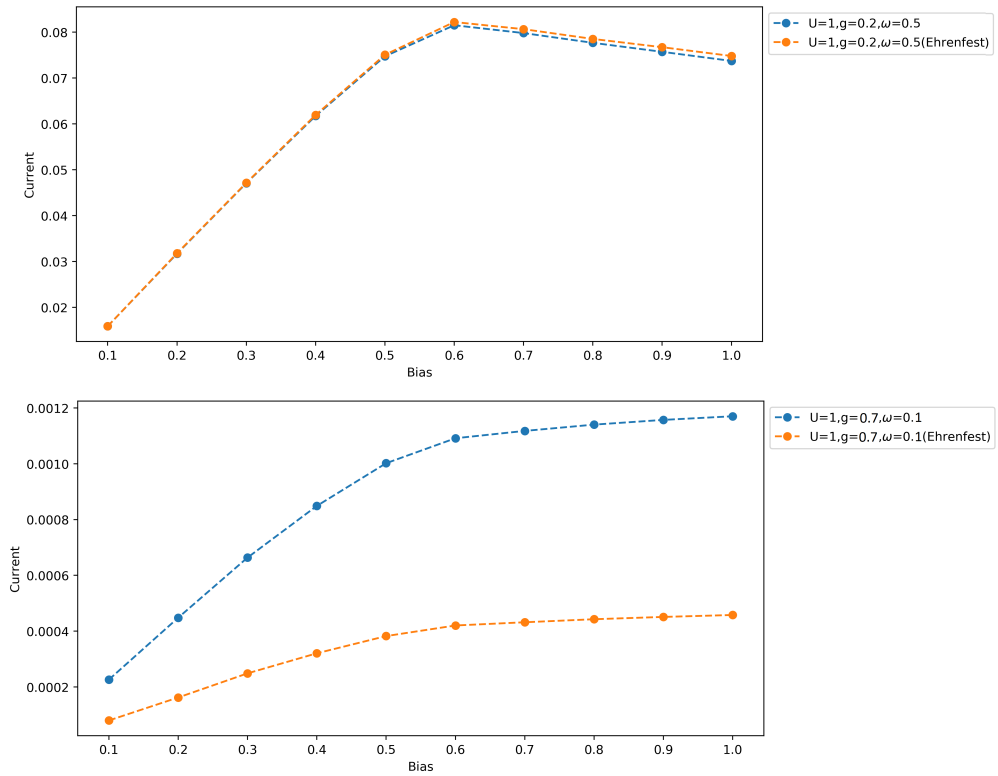

Figure 13: *Steady state current as a function of the bias for two set of parameter where the Ehrenfest approach is compared to DFT.*

4 Conclusions and outlook

In this section the results are briefly summarized and discussed, as well as ideas and plans on how to proceed forward with further investigations. In this thesis we investigated the quantum transport properties across a Hubbard-Holstein junction using Density Functional Theory.

With the code developed during this project we were able to reproduce benchmark results. The steady state transport results were recreated for a purely electronic system [11] and the accuracy of the Verlet algorithm tested. The code was successfully compared with the one used in a paper on the DFT study of a Hubbard Holstein system [18]. This comparison gave a small difference between the two results which is caused by the Verlet algorithm.

We have found that the current through the junction does not increase linearly with the bias, but has instead a non monotonic behaviour when the bias, applied to one of the leads, exceeds a certain value. For this specific bias, the bottom of one of the leads is over the Fermi level of the other. This negatively affects the conductance.

The conductance of a junction with electron-electron and electron-phonon interaction is mainly affected by the electron-phonon interaction strength. We note however that this conclusion refers to the situation, addressed in this thesis, where the impurity density is away from the half filling case; at half-filling, strong e-e effects are expected to occur, since the system enters the Coulomb blockade regime.

With a strong electron-phonon interaction the steady state current has a small value especially if the frequency of oscillation is small. This is mainly caused by the attractive potential created by the phonon displacement which for these parameters is very large. The electron-electron interaction strength does not have a major effect on the steady state current but mostly influences the fast oscillations in the transient period.

We also found clear that if the phonon is treated within the Ehrenfest approximation, the accuracy of the results depends on the frequency. For large frequencies the Ehrenfest scheme provides a good approximation to the steady state current, while for small frequencies the difference between a full DFT approach and the Ehrenfest one is very large.

There are several ways this work can proceed further: On the methodological side, an obvious first step is to connect the impurity to semi-infinite leads and to find the phonon displacement by solving the KS equation for it instead of using the Verlet algorithm. Also, one could proceed to direct determination of the steady state via the Landauer formula, and even determine the condition for the existence of the steady state. Adding complexity, one should consider dynamical corrections to the conductance, and the role of the exchange-correlation bias in the leads.

On the application side, one could consider to explore the Coulomb-blockade regime, the role of more HH impurities and disorder, how results depend on the inter-impurity distance, or how the current can be manipulated by time-dependent gate voltages which can be tuned against phonon frequencies. The possibility of studying thermal phenomena is also within the scope of the method, and so are the conceptual aspect related to the entanglement between electrons and phonons, or between phonons at different impurities. Finally, for more impurities, the possibility of regimes with negative friction could be characterized.

References

[1] W. Kohn and P. Hohenberg. *Phys.Rev.Lett.* **136**, B864 (1964)

[2] W. Kohn and L. J. Sham. *Phys.Rev.Lett.* **140**, A1133 (1965)

[3] E. Runge and E. K. U. Gross *Phys.Rev.Lett.* **52**, 997 (1984)

[4] O. Gunnarsson and K. Schönhammer, *Phys.Rev.Lett.* **56**, 1968 (1986).

[5] N. A. Lima, M. F. Silva, L. N. Oliveira and K. Capelle, *Phys.Rev.Lett.* **90**, 146402 (2003).

[6] F. Aryasetiawan, O. Gunnarsson, A. Rubio, Europhys. Lett. **57**, 683 (2002)

[7] C. Verdozzi, Phys. Rev. Lett. **101**, 166401 (2008).

[8] A. Lanzara, P. V. Bogdanov, X. J. Zhou, S. A. Kellar, D. L. Feng, E. D. Lu, T. Yoshida, H. Eisaki, A. Fujimori, K. Kishio, J.-I. Shimoyama, T. Noda, S. Uchida, Z. Hussain, and Z.-X. Shen. *Nature* 412:35087518 (2001).

[9] A. S. Alexandrov *arXiv*:0408622 (2005)

[10] T. Gunst, T. Markussen, K. Stokbro, M. Brandbyge. *Phys.Rev.Lett.* B **93**, 035414 (2016)

[11] N. Bushong, N. Sai, M. Di Ventra *arXiv*:0504538 (2005)

[12] A. V. Nazarov, Y. M. Blanter. "Quantum Transport: Introduction to Nanoscience." Cambridge, UK (2009)

[13] S. Kurth, G. Stefanucci, E. Khosravi, C. Verdozzi, and E. K. U. Gross*Phys. Rev. Lett.* **104**, 236801 (2010)

[14] S. Kurth, G. Stefanucci, C.-O. Almbladh, A. Rubio, and E. K. U. Gross, Phys. Rev. B **72**, 035308 (2005)

[15] W. Z. Shangguan, T. C. Au Yeung, Y. B. Yu, and C. H. Kam Phys. Rev. B **63**, 235323 (2001)

[16] M.Ya. Azbel "Generalized Landauer formula", Phys Lett. A ,Volume 78, Issue 4 (1980) pp. 410-412.

[17] G. Stefanucci and S. Kurth, *Phys. Rev. Lett.* **107**, 216401 (2011)

[18] E. Viñas Boström, P. Helmer, P. Werner, C. Verdozzi. *arXiv*,1903.04984 (2018)

[19] D. Frenkel, B. Smit . "Understanding molecular simulation: from algorithms to applications", 2. ed., Academic, San Diego, Calif. (2002) pp. 76-77

[20] V. Vettchinkina, A. Kartsev, D. Karlsson, and C. Verdozzi *Phys. Rev. Lett.* B **87**, 115117 (2013)

[21] C. Verdozzi, G. Stefanucci, and C.-O. Almbladh, *Phys.Rev.Lett.* **97**, 046603 (2006)

[22] N. Bode, S. V. Kusminskiy, R. Egger and F. von Oppen, *Phys.Rev.Lett.* **107**, 036804 (2011)